


Application of Levenberg-Marquardt Backpropagation Algorithm in Artificial Neural Network for Self-Calibration of Deflection Type Wheatstone Bridge Circuit in CO Electrochemical Gas Sensor

Amirhosein Asilian^{1,2}, S. Mohammadali Zanjani^{1,2}

1- Department of Electrical Engineering, Najafabad Branch, Islamic Azad University, Najafabad, Iran.
Email: ah.asilian@sel.iaun.ac.ir

2- Smart Microgrid Research Center, Najafabad Branch, Islamic Azad University, Najafabad, Iran.
Email: sma_zanjani@pel.iaun.ac.ir (Corresponding author) 

ABSTRACT:

The unique properties of carbon monoxide and its high combustibility have led to the creation of various sensors, such as electrochemical sensors and different circuits, to read its output. In this article, a deflection-type Wheatstone bridge is used to measure changes in the sensor resistance, and the output voltage is connected to a 12-bit analog-to-digital converter through an adjustable precision amplifier. Next, a new method is proposed for self-calibrating the CO sensor. The Levenberg-Marquardt backpropagation algorithm (LMBP) is utilized in the Artificial Neural Network model to minimize the Mean Squared Error (MSE) and identify the most suitable parameters in the proposed method. The model under consideration has been developed and trained using real-time data. Based on the experimental and evaluation outcomes, it can be concluded that the suggested model has an MSE value of 0.28249 and an R^2 coefficient of determination of 0.99992, indicating high accuracy and precision. The proposed sensor and calibration method have potential applications in various applications, including industrial and domestic environments where CO monitoring is necessary.

KEYWORDS: Electrochemical Sensor, CO Monitoring, Levenberg-Marquardt Backpropagation Algorithm, Mean Squared Error, Training-Validation and Testing (TVT), Coefficient of Determination.

1. INTRODUCTION

Metal oxide gas sensors are essential elements in industrial applications. The sensor output measurement system should be able to create accurate measurement data in the minimum possible calibration time and overcome non-linear output signals [1, 2]. Conventional calibration methods are typically conducted manually and repeatedly, resulting in a time-consuming process [3, 4]. Moreover, these methods are often specific to a particular sensor and cannot be applied to a general measurement system. Consequently, certain sensor parameters may change due to hysteresis, efficiency fluctuations, and nonlinearity, which adversely affect the accuracy of the calibrated output data [2, 5, 6].

The improved accuracy and precision in estimating gas concentrations in monitoring industrial and residential environments have significant practical implications in the following areas: safety, compliance with regulations and standards, energy efficiency, and proactive maintenance [7].

©The Author(s) 2024

Paper type: Research paper

<https://doi.org/10.30486/mjee.2023.1988651.1157>

Received: 19 September 2023; revised: 14 October 2023; accepted: 25 November 2023; published: 1 March 2024

How to cite this paper: A. Asilian, S. Mohammadali Zanjani, “Application of Levenberg-Marquardt Backpropagation Algorithm in Artificial Neural Network for Self-Calibration of Deflection Type Wheatstone Bridge Circuit in CO Electrochemical Gas Sensor”, *Majlesi Journal of Electrical Engineering.*, Vol. 18, No. 1, pp. 21-32, 2024.

In the realm of safety, the proposed self-calibration method, with its more reliable measurements, can aid in identifying and alerting users to hazardous levels of target gas. This enables users to take preventative actions, such as adjusting ventilation systems or implementing strategies to reduce CO levels [8]. Additionally, the increased precision provided by the self-calibration method can facilitate the adherence to regulations and standards. Accurate monitoring of carbon monoxide is crucial for optimizing combustion processes, minimizing energy waste, and improving environmental conditions. The enhanced accuracy can contribute to better energy efficiency and reduced environmental impact. In the context of proactive maintenance, the improved precision from the self-calibration method can assist in the early detection of deviations and potential sensor failures. Continuous monitoring and self-calibration of the CO sensor allow for the swift identification of deviations from expected responses, enabling timely maintenance and troubleshooting [9].

Smart sensors implement various calibration algorithms, including recursive algorithms [10, 11] and those based on neural networks [2, 12]. Neural networks offer a reliable means to model and predict complex problems [13-16]. Currently, neural networks are utilized to identify the sensor's transfer function (T.F) response curve and linearize the input-output relationship [17, 18]. Neural networks are versatile tools that can be utilized to tackle a broad range of problems and tasks, including but not limited to classification, interpretation, detection, modeling, and control. They are particularly useful for addressing problems that are too intricate to be tackled by traditional mathematical modeling or other conventional methods. The ability of neural networks to learn and generalize from data makes them an effective and efficient solution for many real-world problems [19]. Before designing any Artificial Neural Network (ANN), there are some essential considerations. Equation (1) defines the relationship between the measured input variable and the electrical output signal of the sensor.

$$x' = f(v') \quad (1)$$

Where, x' is the electrical output signal, v' is the input variable, and f is the T.F of the sensor.

Gas sensor input and output variables typically have dissimilar scales and are often normalized between 0 and 1 using equations (2) for the sake of simplicity [2].

$$x = \frac{x' - x'_{min}}{x'_{max} - x'_{min}} \quad v = \frac{v' - v'_{min}}{v'_{max} - v'_{min}} \quad (2)$$

Where, v' and x' are the input and output variables, respectively, and v'_{min} , x'_{max} , x'_{min} and x'_{max} are the minimum and maximum values of the input and output variables, respectively. The normalized variables are denoted by v and x .

The objective is to minimize the Mean Squared Error (MSE) between the desired target signal, t , and the output signal, y , in order to achieve a straight line with a unit slope, as depicted in Fig. 8, as part of the ideal calibration process. The ANN's ability to linearize the output signal (y) is determined based on the minimum MSE, as outlined in equation (3).

$$\varepsilon_{MSE} = \frac{1}{N} \sum_{n=1}^N (y_n - t_n)^2 \quad (3)$$

Here, N stands for the number of data points, t represents the target signal, and y denotes the output signal of the ANN. Equation (4) defines the logsig function, a frequently employed activation function in artificial neural networks. This function, along with other activation functions such as Gaussian, sigmoid, and ramp functions, is widely used to enable ANNs to solve complex problems. It is worth noting that the logsig function constrains the output range to (0~1).

$$\text{logsig}(x) = \frac{1}{1 + \exp(-x)} \quad (4)$$

Where, x is the input to the function, and $\exp(-x)$ is the exponential function of $-x$.

In [20, 21], ANN topologies such as Multi-Layer Perceptron (MLP) and Radial Basis Function (RBF) have been evaluated. Both types of networks have the ability to approximate functions. Although it is clear that RBF is a good function approximation system, compared to the RBF network, the MLP is a relatively straightforward approach. Moreover, the RBF network is entirely computational in nature [22, 23]. However, the main role of successful algorithm training is to minimize MSE, increase convergence speed, and select an appropriate learning rate. Levenberg-Marquardt Backpropagation (LMBP) is a variation of the Newtonian method and uses the backpropagation process. This method is designed to minimize non-linear functions that are the sum of other non-linear functions'

squares. Additionally, it can decrease the sum of squares in each iteration by utilizing a specific approach [24]. A flowchart outlining the steps of this algorithm can be found in reference [2]. This method is suitable for training neural networks where the performance index is Mean Squared Error. The structure of the article includes the following sections. In Section 2, the specifications of the gas sensor used are briefly reviewed. The electronic circuit design for reading the output is also discussed in this section. Section 3 focuses on the proposed neural network for calibration. Section 4 will delve into the results acquired from the design's implementation, while Section 5 will offer a synopsis of the conducted work.

2. GAS SENSOR SPECIFICATIONS AND OUTPUT READING CIRCUIT

For the gas sensor designed and manufactured in Fig. 1a with 27.5 sec response time and 39 sec recovery time, the results of measurements at a temperature of 250°C are shown in Fig. 1b, which indicates the changes in sensor resistance as a function of applied gas concentration. If R_a represents the sensor resistance in ambient air and R_g represents the resistance in the presence of the target gas, the sensor resistance without the target gas (exposed to air) was measured at 169 KΩ with an output voltage of 720.58 mV. However, in the test with a concentration of 470 ppm, the sensor resistance was measured at 1.12 KΩ and the output voltage was 2876.18 mV. Using a 12-bit Analog to Digital Converter (ADC) unit and an STM32F107VC microcontroller with a resolution of 0.805 μV, the output voltage was measured using the proposed reading circuit.

Fig. 2 shows the deflection-type Wheatstone bridge circuit used to measure changes in the sensor resistance. The resistance R_1 is used to adjust the sensitivity of the bridge, and R_2 is the zero-adjustment resistor used for gas sensor calibration. The output voltage of the bridge varies proportionally with the change in the sensor layer conductivity and is connected to the AD623. The circuit is designed in such a way that the low-level bridge output is amplified and converted to a voltage that can be transferred to an ADC. AD623 is an instrumentation amplifier that offers high-precision amplification of small signals. It has a high Common-Mode Rejection Ratio (CMRR) and a low input offset voltage, making it suitable for amplifying small differential signals in noisy environments. AD623 has the advantages of easy gain adjustment and a low loading effect. The gain can be adjusted by changing the R_{Gain} resistor and the gain can be calculated using Equation (5).

$$Gain = \frac{100 \text{ K}\Omega}{R_{Gain}} + 1 \quad (5)$$

With $R_{Gain}=100 \text{ K}\Omega$, the gain is obtained as 2. Using equation (6), the output voltage of the instrumentation amplifier can be calculated differentially.

$$v_0 = Gain(v_2 - v_1) \quad (6)$$

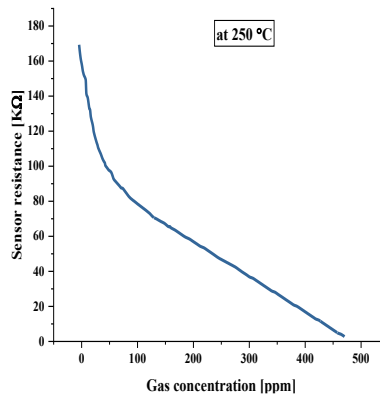


Fig. 1. a) The employed CO gas sensor. b) Changes in the sensor resistance as a function of the applied gas concentration to the sensor [۷۵].

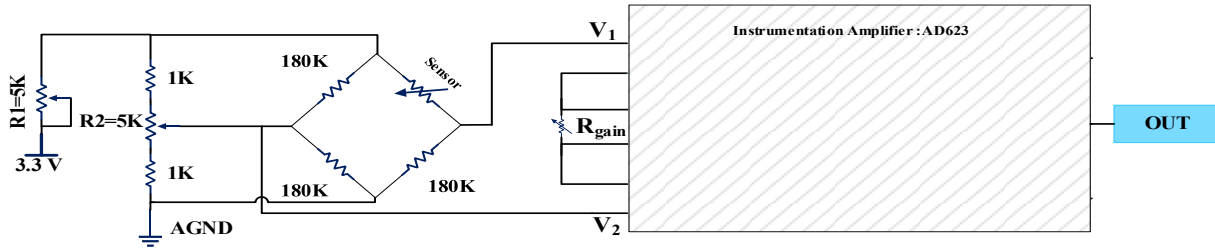


Fig. 2. Circuit for readout and amplifying the output signal of the sensor.

3. CALIBRATION AND PROPOSED ANN ARCHITECTURE

The traditional calibration methods, which involve manual and often repetitive processes, can be time-consuming depending on the required accuracy of the sensor measurement. The current section provides an overview of the implementation of an ANN model for the self-calibration of the gas measurement system. Along with this, the training algorithm parameters of the model are described in detail. To evaluate the response and calibration, first, the sensor is placed in a chamber. Then, the heater temperature is set and the system is allowed to stabilize to the measured response. The raw values read by the ADC are then stored and used for neural network training. The block diagram of the testing and data collection system is illustrated in Fig. 3.

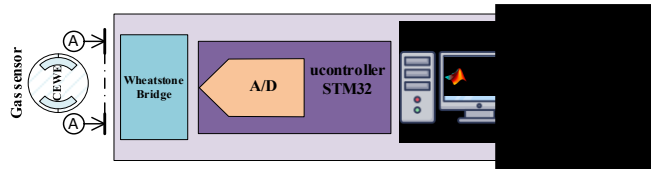


Fig. 3. Block diagram of the testing and data collection system.

In order to improve the calibration time and accuracy of gas sensors used in real-time measurement systems, it is recommended to incorporate a self-calibration algorithm during their development. This is particularly important for electrochemical sensors since their sensitivity and linearity can decrease over time due to chemical reactions between the sensor surface and the environment. By using a self-calibration algorithm, the sensor can be optimally utilized and maintained in the best possible condition. Optimizing the architecture of an artificial neural network lacks a widely accepted method, thus a trial-and-error approach was employed based on the method put forth in [18]. Throughout the design process, various features such as the number of layers, neurons, training algorithms, activation functions, and computational requirements were taken into account. The objective was to create an ANN structure that would result in the lowest possible output error while maintaining simplicity. The network architecture was initially designed with a small number of hidden neurons, which were later modified based on the outcomes achieved. Fig. 4 shows the proposed ANN model architecture that offers excellent generalization. The network is composed of several layers of neurons, each having a non-linear transfer function. This feature allows the network to learn and comprehend both linear and non-linear relationships between input and output vectors. The non-linear transfer functions are crucial because they enable the network to model complex relationships that exist in the data. The network's ability to capture both linear and non-linear relationships is essential for its effectiveness in applications such as pattern recognition and classification. This feature makes the network capable of processing and interpreting data inputs, regardless of their complexity, to produce the desired output. The proposed ANN model includes an input node that represents the various parameters that affect the gas sensor's calibration. The hidden layer of the network comprises eight neurons with a logarithmic activation function, while the output layer consists of a single neuron with a linear activation function. This neuron is responsible for representing the gas pattern in the self-calibration process. The output of the ANN is defined by Equation (7).

$$y = \text{Purelin} \left[w_i^2 \left(\text{Logsig} \left(w_i^1 x + b_i^1 \right) \right) + b_i^2 \right] \quad (7)$$

$$i = 1 \text{ to } 8$$

In equation (7), x denotes the normalized output signal, while y denotes the linearized or uncalibrated signal. The vector w represents the weights of the network, while b denotes the bias.

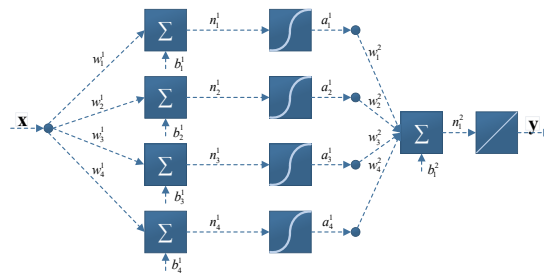


Fig. 4. The architecture of the ANN used.

After conducting a thorough analysis, it was determined that the MLP feedforward model with the LMBP training algorithm was the most fitting approach for the task at hand. To ensure that the calibration data was unbiased, it was randomly divided into three subsets, namely training, test, and validation subsets. This approach allowed for a more comprehensive evaluation of the model's performance. The traditional training validation testing approach is adopted to optimize the ANN model. The training set plays a crucial role in determining the structure of the model and computing the ANN weights and biases. The primary objective of this process is to minimize the error function and augment the accuracy of the model with each iteration. The validation set is employed to prevent overfitting and identify the optimal set of parameters, which provides an unbiased evaluation of the generalization error of the model. On the other hand, the test set is solely utilized to assess the performance of the trained model, providing a reliable measure of its effectiveness. The training process continues until the validation error is unsuccessful. The values of the parameters employed in the artificial neural network model and their corresponding properties are demonstrated in Table 1.

Table 1. Properties and parameters of the proposed ANN model.

Training parameters	Values
Model of neural network	Feedforward
Transfer function output layer	Pure line
Transfer function hidden layer	Logsig
Input nodes	1
Hidden layer neurons	8
Hidden layer	1
Output nodes	1
Algorithm for network training	LMBP
Testing percentage	15
Training data Percentage	70
Output layer neurons	1
Validation percentage	15
Number of epochs	384
Validation checks (iterations)	6
Performance	0.28249

MATLAB software was utilized to implement the proposed method for training and output computation. The process of training the model and calculating the output was carried out through the use of this software. This allowed for the efficient execution of the proposed method and helped to ensure that the results obtained were accurate and reliable. The training of the proposed model updates the weights between neurons as per equation (7), where the ANN outputs are calculated by combining biases and weights. Each time an ANN is trained, it may result in a new solution due to various factors such as the initial values of weights and the allocation to training, validation, and testing (TVT) sets of data. This means that the output generated by different ANNs for the same input to solve a particular problem may not be consistent. The variation in the output can occur due to differences in the neural network architectures, training techniques, and the initial weights assigned to the connections between neurons in the network. To guarantee high accuracy in ANN training, this study employed a trial-and-error approach, training the network multiple times. The results presented in the subsequent section represent the best output after several training sessions.

The training output was continually updated at each iteration to achieve the best performance by reaching the minimum MSE, signifying the successful implementation of a self-calibration method.

4. RESULTS OF THE PROPOSED NEURAL NETWORK TRAINING AND EVALUATION

In this section, the experimental and analytical results of the gas sensor-based measurement system will be discussed. The results of the performance of the calibration algorithm that is implemented are comprehensively analyzed and interpreted.

Furthermore, the investigation into the performance of the ANN model is evaluated. This model aims to provide a thorough evaluation of the gas sensor-based measurement system and the associated calibration algorithm. In addition, a detailed analysis of the effectiveness and efficiency of the model is presented.

The dynamic calibration process involves calibrating measurements that vary over time. For this purpose, a chamber, a shut-off valve, and a calibrated gas capsule were employed in the proposed design to expose the sensor to gas continuously, enabling instant readings and storage of standard values. However, precise measurement data from the gas sensor is crucial to obtain acceptable results. Therefore, the relationship between the read voltage, which is proportional to changes in the sensor resistance, and the applied gas concentration must be learned. The sensor's performance was evaluated over the given, and the calibration process was repeated several times. During this evaluation, errors caused by non-linearity, hysteresis, and non-repeatability were identified. The relative change in the measured voltage during the test indicates the presence of errors such as changes in gain, non-linearity, and hysteresis, which can adversely impact the measurement system. Fig. 5 illustrates the behavior of the output voltage as a function of gas concentration under ideal and measured conditions. Fig. 5 shows that in the presence of CO gas, the sensor's resistance initially decreases due to the release of free electrons, causing an increase in the output voltage. However, it eventually saturates depending on the type of electrochemical sensor structure.

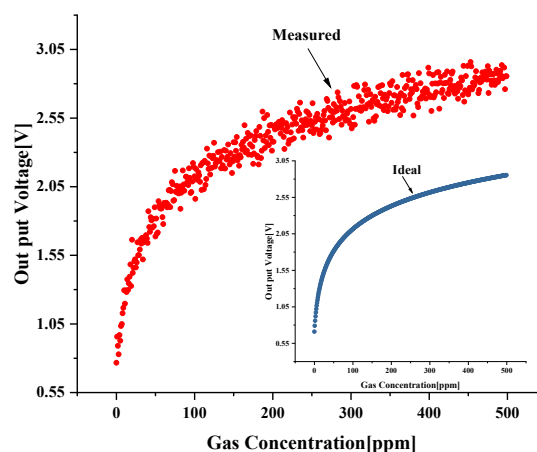


Fig. 5. Graph of changes in the output voltage of the gas sensor as a function of the density of CO gas applied to the sensor in two expected and measured states.

In the proposed method, an ANN was implemented with some modifications using the Levenberg-Marquardt backpropagation (LMBP-ANN) algorithm in the MATLAB Neural Network toolbox. The feedforward networks are usually trained by using the backpropagation algorithm. In LMBP, the data goes from the input to the hidden and then to the output layer. The error signal at the output layer is sent back to the hidden and input layers. The connection weights are adjusted to minimize the sum of squares of the error. As data generation is essential in the training algorithm, Data was gathered from the measurement system using a gas sensor and an interface board, with gas chromatography utilized as a reference for calibration data. More than 15,000 calibration data points were obtained to train the gas sensor ANN, with dynamic calibration conducted as well. The proposed ANN model structure is depicted in Fig. 6.

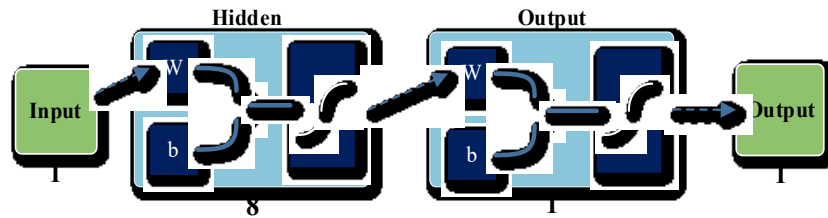


Fig. 6. Feedforward network (Logsig T.F and a linear T.F in the hidden layer and the output layer).

The training process was carried out until the network achieved the best validation performance. Fig. 7 displays the changes in the Mean Squared Error (MSE) throughout the training stages. The TVT errors declined consistently until the validation error stopped decreasing after six iterations, and the validation process was halted. During this training, the network attained the best MSE at stage 378, which is a logical outcome for several reasons: the final performance was low, at 0.28249; the validation set error and test set error had similar properties, and there was no substantial overfitting at stage 378, which coincided with the best validation performance.

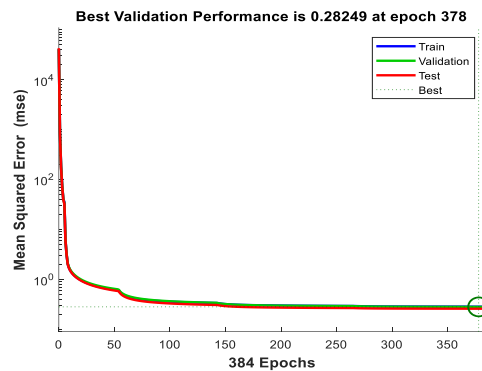


Fig. 7. Performance of TVT errors consisting of training epochs.

5. PERFORMANCE OF LMBP-ANN MODEL

The performance of the ANN model primarily depends on the accuracy of the model's prediction of laboratory output data. Fig. 8 demonstrates that the output of the ANN model can precisely predict gas self-calibration compared to Empirical measurements data. For instance, the R^2 coefficient of determination against the experimental data for the TVT are 0.99992, 0.99991, and 0.99991, respectively. The proposed ANN model has demonstrated its efficacy in capturing the intricate and multifaceted relationships that exist between the input and output data. The ANN model has proven to be a powerful tool for modeling complex systems, as it is capable of learning and adapting to the underlying patterns and structures of the data. By leveraging the principles of machine learning and statistical analysis, the ANN model has been able to effectively capture the nuances of the input and output data, resulting in a highly accurate and reliable predictive model. Overall, the proposed ANN model represents a significant advancement in the field of data analysis and modeling. The model has exhibited exceptional performance in precisely and comprehensively processing and interpreting the input data, resulting in the production of the intended outputs. This exemplary performance serves as a testament to the system's efficacy and efficiency, further highlighting its impressive capabilities. To evaluate the effectiveness of the LMBP-ANN model proposed in this study for the entire dataset, the model's predictions were compared to experimental results, and both the MSE and R^2 coefficient are calculated. The MSE was determined to be 0.28249 using formula 3, and the R^2 value was calculated to be 0.99992, indicating good performance.

$$\begin{aligned}
 w^1 &= [-33.8089 \quad -1.3363 \quad -6.6277 \quad 7.3073 \quad 1.7907 \quad 7.2151 \quad -9.3117 \quad -10.9006] \\
 b^1 &= [32.1993 \quad 2.6160 \quad 3.4751 \quad -2.2077 \quad -0.2122 \quad 2.6985 \quad -5.7544 \quad -9.2788] \\
 w^2 &= [-0.0008 \quad -13.4417 \quad -0.0027 \quad 0.0013 \quad 0.0359 \quad 0.0011 \quad -0.0013 \quad -0.0012] \\
 b^2 &= [12.4751]
 \end{aligned} \tag{8}$$

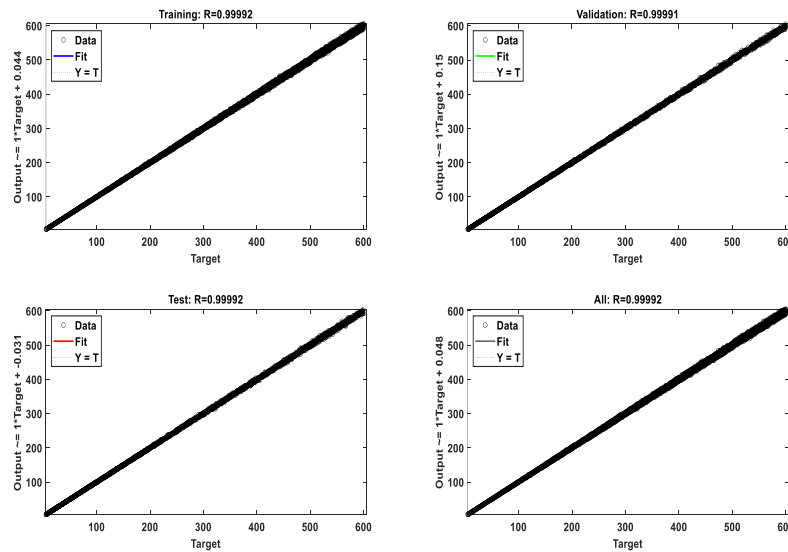


Fig. 8. The compromise between the output gas concentration of the network and the target for training, validation, testing, and complete dataset.

To further verify the performance of the network, the histogram method was utilized. The distribution of data for a continuous variable is shown in Fig. 9, with the blue, green, and red bars representing the TVT data, respectively. The histogram can identify outliers, where data points deviate significantly from the major part of the acquired data. In this instance, the error histogram implies that they are often between -1 and 1, and based on the test regression plot, no outliers were present. As a result, there was no need to collect additional data.

The bias and weight matrices for the trained ANN at epoch 384 are displayed and saved for use in programming microcontrollers to determine gas compensation. In equation set (8), w^1 refers to the input hidden-layer connection weights, and w^2 stands for the output hidden-layer connection weights. Additionally, b^1 and b^2 are employed to determine the bias value of both layers, respectively.

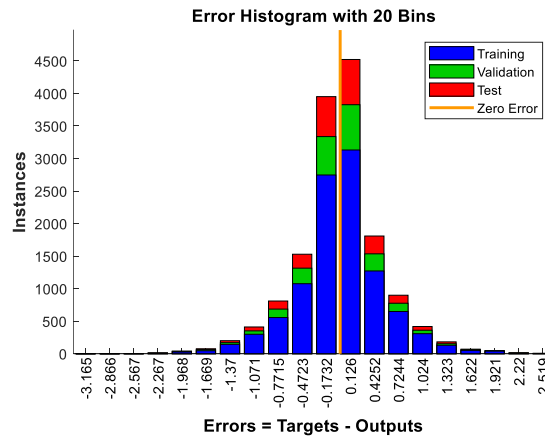


Fig. 9. Histogram of 20 Bins using the LMBP training based on the proposed Neural Network.

To evaluate the efficiency of the trained neural network, a new and independent input data set was employed, which was not included in the algorithm during the training phase. The neural network was tasked with predicting gas calibration based on a new vector consisting of 2000 input data points. These data points were proportional to the gas concentration measured by the Wheatstone bridge circuit and were used to create a voltage vector. The trained neural network was then able to process this new input data and generate predictions for the gas calibration. This approach helped to validate the accuracy of the neural network's predictions on new and independent data. The voltage data with values ranging from 0.72 to 2.89 volts were fed into the ANN. As depicted in Fig. 10, the LMBP-ANN model accurately predicted gas self-calibration compared to the target gas. This suggests that the neural network, which has been trained, is capable of accurately measuring and correcting gas input.

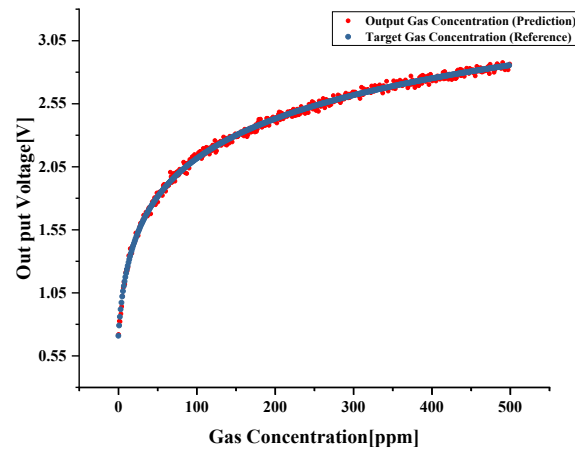


Fig. 10. Output of the trained ANN compared to the target (reference) using input from the dataset that was not used for training.

6. COMPARISON WITH PREVIOUS WORKS

In Table 2, a comprehensive comparison has been made between the performance of prior studies in gas sensor applications and the innovative design proposed in this work. It is worth noting that, in most previous works, instances similar to this paper, focusing on the development of neural network algorithms for gas concentration estimation and self-calibration of gas sensors, have rarely been observed.

In [26, 27], the Partial Least Squares (PLS) regression algorithm, which is a statistical method, has been employed. PLS is a multivariate regression technique used for predicting gas concentrations and chemical data. One of the challenges of this method is the complexity of interpretation, as it involves linear combinations of independent variables, making it difficult to interpret them for a precise understanding of the relationships between variables. Furthermore, it is not suitable for small datasets and requires various settings, such as the number of components. Sensitivity to outliers and data distribution dependency are also disadvantages of this method. This approach has been used in [26, 27], resulting in a Root Mean Square Error (RMSE) of 7.34 in gas concentration prediction.

In [28], the Multilayer Perceptron Neural Network algorithm has been utilized for gas concentration estimation. This method offers high generalization capability with an appropriate number of layers and hidden neurons, resilience to noisy features, and high flexibility. The use of this approach has led to a reduction in error rates, ranging from 7% to 19% in the worst-case scenario compared to other methods. However, it comes with drawbacks such as the need for proper initialization, complexity in parameter tuning, difficulty in interpreting the resulting models, and the time-consuming nature of training.

In [29], another powerful machine learning algorithm called Extreme Gradient Boosting method (XGBoost) has been employed. The XGBoost is widely used in classification challenges. Its advantages include high accuracy and predictions achieved by combining decision trees and gradient boosting. Its resistance to overfitting results in better model generalization. Although this algorithm can handle noisy data, work with large datasets, and support various types of features, including numerical and ordinal features, using XGBoost in [29] improved the accuracy in classification to 96.62% and sensitivity to 95.6%. However, it comes with drawbacks such as the need for parameters tuning, longer training times compared to some simpler algorithms, and complexity in model interpretation compared to some simpler methods.

The K-Nearest Neighbors (KNN) algorithm is an instance-based machine learning algorithm used in classification and regression tasks. It is sensitive to noise, and consumes significant computational resources (memory and time), especially when dealing with a large number of samples. Additionally, the choice of the parameter K (the number of neighbors) is crucial, and selecting the wrong value for K can lead to suboptimal accuracy in predictions. However, in [30], this method has been used for drift compensation, resulting in an accuracy ranging from 80.74% to 97.5%.

OPLS is a method belonging to the PLS family. This algorithm is used for modeling the relationships between dependent and independent variables in multivariate data. The key feature of OPLS is that it separates information that may be incorrect or present in independent variables from the output (prediction) equation. In [31], OPLS has been used to improve accuracy up to 91%.

PLS-DA is a type of discriminant analysis used for data classification problems. This algorithm, similar to PLS, focuses on decomposing a linear combination of independent variables to predict dependent variables. However, in

PLS-DA, the main goal is data classification. In [32], the PLS-DA method has been employed for the same purpose, and it has also improved accuracy to 91%.

The performance of domain transfer depends on the selection of the source and target domains and the appropriate alignment of data. Given the changes in data distribution in the new domain, transfer can be achieved from one domain to another using techniques such as data distribution alignment, feature alignment, and domain feature alignment. Using these methods in [33, 34] results in average accuracy ranging from 79.4% to 95.92%.

In [35], a new discriminative method based on unsupervised Domain Adaptation (DA) has been introduced to address the gas sensor drift problem. In this paper, a novel DA with Neighborhood Preserving (DANP⁺) is presented, which incorporates subspace learning capabilities into classifier training. A weight allocation function is introduced to assign different weights to different subspace dimensions. In this paper, average accuracy has reached a range of 77.83% to 79.76%.

Nevertheless, it is a common practice to use multiple evaluation methods, such as cross-validation, to select the best model. Additionally, combining different models as an ensemble architecture may lead to improved performance. Overall, it should be noted that algorithms based on machine learning have complexity in calculations and interpretation of information. Also, implementing these methods in a portable and industrial system often requires expensive and powerful hardware. However, the method presented in this paper has achieved an MSE value of 0.28249 and an R² value of 0.99992. Furthermore, as shown in Fig. 10, the evaluation of the neural network in gas concentration prediction demonstrates the high accuracy of the proposed neural network. The proposed neural network uses a small number of hidden layers and neurons, making it easier to implement on common hardware such as microcontrollers.

7. CONCLUSION

In this article, a new method for estimating gas sensor self-calibration has been proposed to create reliability for the long-term use of electrochemical gas sensors. The proposed method for gas concentration estimation was implemented using the LMBP-ANN model, a neural network architecture that employs the LMBP training algorithm to minimize mean square error and determine optimal parameters. Real-time experimental data from the gas measurement system were collected and utilized to train the developed ANN model. The obtained results from the experiments indicate that the ANN model exhibits high precision in forecasting gas concentration, surpassing traditional approaches in the context of real-time estimation accuracy. To determine the effectiveness of the proposed model, a comprehensive analysis was conducted of the entire dataset. The evaluation was carried out by comparing the model's predictions against the actual experimental results using two metrics: the MSE and the R² coefficient of determination. The MSE value obtained was 0.28249, indicating that the average difference between the predicted and actual values was quite low. Similarly, the R² value was found to be 0.99992, which suggests that the model's predictions were highly accurate and reliable. These results indicate that the proposed model performed exceptionally well in predicting the outcomes of the experiments, and can be deemed a valid tool for future research in this field.

It is important to acknowledge the limitations of the based on AI methods, including:

- i. Dependency on Laboratory Conditions: Neural network-based methods typically require specific training data and laboratory conditions. As a result, this method may perform optimally only under specific laboratory conditions.
- ii. Sensitivity to Environmental Conditions: The performance of the electrochemical CO gas sensor may be highly sensitive to environmental factors such as temperature, humidity, and pressure. If this method has been developed exclusively under specific laboratory conditions, it may exhibit reduced accuracy in real-world settings and variable environments.
- iii. Computational Complexity: The use of the LMBP-ANN neural network for self-calibration may entail complex and time-consuming computations. These computations could impose limitations on real-time operations or deployment in embedded systems.

Table 2. Comparison of Gas Sensor Algorithm Performance.

<i>Algorithms</i>	<i>Applications</i>	<i>metrics Performance</i>	<i>References</i>
PLS	Gas concentration prediction	RMSE: 7.34	26, 27
MLPNN	Gas concentration estimation	Error decreased 7%–19% worst case	28
XGBoost	Classification	Accuracy: 96.62%, Sensitivity: 95.60%, Specificity: 91.09%	29

KNN	Drift compensation	Accuracy: 80.74%–97.5%	30
OPLS	Drift suppressed classification	Accuracy: 91%	31
PLS-DA	Drift suppressed feature augmentation	Accuracy: 91%	32
Domain transfer	Drift and interference suppression	Avg accuracy: 79.4%–95.92%	33,34
DANP & DANP+	Drift suppressed classification	Avg accuracy: 77.83%–79.76%	35
LMBP	Gas concentration prediction and estimation	MSE: 0.28249 R ² : 0.99992	This work

Data Availability. Data underlying the results presented in this paper are available from the corresponding author upon reasonable request.

Funding. There is no funding for this work.

Conflicts of interest. The authors declare no conflict of interest.

Ethics. The authors declare that the present research work has fulfilled all relevant ethical guidelines required by COPE.



This article is licensed under a Creative Commons Attribution 4.0 International License.

©The Author(s) 2024

REFERENCES

- [1] J. Rivera, G. Herrera, M. Chacón, P. Acosta, and M. Carrillo, “Improved Progressive Polynomial Algorithm for Self-Adjustment and Optimal Response in Intelligent Sensors,” *Sensors*, Vol. 8, No. 11, pp. 7410-7427, 2008.
- [2] J. Rivera, M. Carrillo, M. Chacón, G. Herrera, and G. Bojorquez, “Self-Calibration and Optimal Response in Intelligent Sensors Design Based on Artificial Neural Networks,” *Sensors*, Vol. 7, No. 8, pp. 1509-1529, 2007.
- [3] S. M. A. Zanjani, M. Aalipour, and M. Parvizi, “Design of a Low Power Temperature Sensor Based on Sub-Threshold Performance of Carbon Nanotube Transistors with an Inaccuracy of 1.5 °C for the range of -30 to 125°C.” *Journal of Intelligent Procedures in Electrical Technology*, Vol. 13, No. 50 pp. 115-127, 2022.
- [4] G. Farias *et al.*, “A Neural Network Approach for Building An Obstacle Detection Model by Fusion of Proximity Sensors Data,” *Sensors*, Vol. 18, No. 3, p. 683, 2018.
- [5] J. R. Rivas, F. Lou, H. Harrison, and N. Key, “Measurement and calibration of centrifugal compressor pressure scanning instrumentation,” 2015.
- [6] A. Sharafat, *et al.* “Low-Cost CO Sensor Calibration Using One Dimensional Convolutional Neural Network” *Sensors*, Vol. 23, No. 2, p854, 2023.
- [7] J. Baranwal, *et al.* “Electrochemical sensors and their applications: A review,” *Chemosensors*, Vol. 10, No. 9, p. 363, 2022.
- [8] V. Tangirala, *et al.* “A study of the CO sensing responses of Cu-, Pt-and Pd-activated SnO₂ sensors: effect of precipitation agents, dopants and doping methods,” *Sensors*, Vol. 17, No. 5, p. 1717, 2011.
- [9] Mallampati, S. B., & Seetha, H. “A Review on Recent Approaches of Machine Learning, Deep Learning, and Explainable Artificial Intelligence in Intrusion Detection Systems,” *Majlesi Journal of Electrical Engineering*, Vol. 17, No. 1, pp. 29-54, 2023.
- [10] K. F. Lyahou, G. van der Horn, and J. H. Huijsing, “A noniterative polynomial 2-D calibration method implemented in a microcontroller,” *IEEE Transactions on Instrumentation and Measurement*, Vol. 46, No. 4, pp. 752-757, 1997.
- [11] J. D. Pereira, O. Postolache, and P. S. Girao, “Adaptive self-calibration algorithm for smart sensors linearization,” *IEEE Instrumentation and Measurement Technology Conference Proceedings*, Vol. 1, pp. 648-652, 2005.
- [12] N. Abu-Khalaf and J. J. L. Iversen, “Calibration of a sensor array (an electronic tongue) for identification and quantification of odorants from livestock buildings,” *Sensors*, Vol. 7, No. 1, pp. 103-128, 2007.
- [13] H. Adeli, “Neural networks in civil engineering: 1989–2000,” *Computer-Aided Civil and Infrastructure Engineering*, Vol. 16, No. 2, pp. 126-142, 2001.
- [14] H. Ghadiri, “Real-time Stability Assessment of Power System using ANN without Requiring Expert Experience,” *Majlesi Journal of Electrical Engineering*, Vol. 14, No. 2, pp. 43-49, 2020.

- [15] S. B. Mallampati, and H. Seetha, "A Review on Recent Approaches of Machine Learning, Deep Learning, and Explainable Artificial Intelligence in Intrusion Detection Systems," *Majlesi Journal of Electrical Engineering*, Vol. 17, No. 1, pp. 29-54, 2023.
- [16] S. M. A. Zanjani, H. Shahinzadeh, J. Moradi, M. Fayaz-dastgerdi, W. Yaïci, and M. Benbouzid. "Short-term Load Forecasting using the Combined Method of Wavelet Transform and Neural Networks Tuned by the Gray Wolf Optimization Algorithm," *Global Energy Conference (GEC)*, IEEE, pp. 294-299, 2022.
- [17] A. Al-Salaymeh, "Optimization of hot-wire thermal flow sensor based on a neural net model," *Applied thermal engineering*, Vol. 26, No. 8-9, pp. 948-955, 2006.
- [18] A. S. Ciminski, "Neural network based adaptable control method for linearization of high power amplifiers," *AEU-International Journal of Electronics and Communications*, Vol. 59, No. 4, pp. 239-243, 2005.
- [19] A. Ramadan Suleiman and M. L. Nehdi, "Modeling self-healing of concrete using hybrid genetic algorithm-artificial neural network," *Materials*, Vol. 10, No. 2, p. 135, 2017.
- [20] Y. H. Hu and J.-N. Hwang, "Introduction to neural networks for signal processing," in *Handbook of neural network signal processing: CRC press*, p. 1, 2018.
- [21] B. Erhan, C. Oral, and E. Ufuk Ergül. "Classification of arithmetic mental task performances using EEG and ECG signals," *The Journal of Supercomputing*, pp. 1-13, 2023.
- [22] A. Depari, A. Flammini, D. Marioli, and A. Taroni, "Application of an ANFIS algorithm to sensor data processing," *IEEE Transactions on Instrumentation and Measurement*, Vol. 56, No. 1, pp. 75-79, 2007.
- [23] A. Depari *et al.*, "Digital signal processing for biaxial position measurement with a pyroelectric sensor array," *IEEE transactions on instrumentation and measurement*, Vol. 55, No. 2, pp. 501-506, 2006.
- [24] A. M. Almassri, W. Z. Wan Hasan, S. A. Ahmad, S. Shafie, C. Wada, and K. Horio, "Self-calibration algorithm for a pressure sensor with a real-time approach based on an artificial neural network," *Sensors*, Vol. 18, No. 8, p. 2561, 2018.
- [25] A. Asilian, S. M. A. Zanjani. "Design and fabrication of an amperometric CO gas sensor and a readout circuit using a low-noise transimpedance amplifier to achieve standard analog outputs," *AEU-International Journal of Electronics and Communications*, Vol. 171, p. 154864, 2023.
- [26] Wozniak, L., Kalinowski, P., Jasinski, G., & Jasinski, P. (2018). "FFT analysis of temperature modulated semiconductor gas sensor response for the prediction of ammonia concentration under humidity interference," *Microelectronics Reliability*, Vol. 84, pp. 163-169, 2018.
- [27] Burgués, J., Esclapez, M. D., Doñate, S., & Marco, S. "RHINOS: A lightweight portable electronic nose for real-time odor quantification in wastewater treatment plants," *IScience*, Vol. 24, No. 12, 2021.
- [28] Wang, J., Lian, S., Lei, B., Li, B., & Lei, S. "Co-training neural network-based infrared sensor array for natural gas monitoring," *Sensors and Actuators A: Physical*, Vol. 335, pp. 113392, 2022.
- [29] Chen, K., Liu, L., Nie, B., Lu, B., Fu, L., He, Z., . & Liu, H. "Recognizing lung cancer and stages using a self-developed electronic nose system," *Computers in Biology and Medicine*, Vol. 131, p. 104294, 2021.
- [30] Srinivasan, P., Robinson, J., Geevaretnam, J., & Rayappan, J. B. B. (2020). "Development of electronic nose (Shrimp-Nose) for the determination of perishable quality and shelf-life of cultured Pacific white shrimp (*Litopenaeus Vannamei*)," *Sensors and Actuators B: Chemical*, Vol. 317, pp. 128192, 2020.
- [31] Bax, C., Prudenza, S., Gutierrez-Galvez, A., & Capelli, L. "Drift compensation on electronic nose data relevant to the monitoring of odorous emissions from a landfill by opls," *Chemical Engineering Transactions*, Vol. 85, pp. 13-18, 2021.
- [32] Valcárcel, M., Ibáñez, G., Martí, R., Beltrán, J., Cebolla-Cornejo, J., & Roselló, S. "Optimization of electronic nose drift correction applied to tomato volatile profiling," *Analytical and Bioanalytical Chemistry*, Vol. 413, No. 15, pp. 3893-3907, 2021.
- [33] Liang, Z., Xue, Q., Tian, F., Xu, C., Wang, C., Yang, L., & Guo, T. "A sparse reconstruction domain transfer method for interference suppression in artificial olfactory system," *IEEE Sensors Journal*, Vol. 22, No. 7, pp. 6717-6730, 2022.
- [34] Zhu, X., Liu, T., Chen, J., Cao, J., & Wang, H. "One-Class Drift Compensation for an Electronic Nose," *Chemosensors*, Vol. 9, No. 8, p. 208, 2021.
- [35] Yi, Z., Shang, W., Xu, T., & Wu, X. "Neighborhood preserving and weighted subspace learning method for drift compensation in gas sensor," *IEEE Transactions on Systems, Man, and Cybernetics: Systems*, Vol. 52, No. 6, pp. 3530-3541, 2021.